https://doi.org/10.1016/j.conbuildmat.2016.12.207

Effects of Material Composition on Mechanical and Acoustic Performance of PoroElastic Road Surface (PERS)

Dawei Wang[1], Andreas Schacht[2], Zhen Leng[3*], Chao Leng[4], Jonas Kollmann[1], Markus Oeser[1]

ABSTRACT

Poroelastic road surface (PERS) is a type of low-noise pavement surface, which was derived from porous asphalt (PA). Because of its high elasticity, large air void content and an inter-connected air void structure, PERS provides excellent performance in traffic noise reduction. However, it also faces the challenging problem of poor ravelling resistance, which limits its more widespread application. The main objective of this study is to investigate the effects of various composition factors on the ravelling resistance of PERS so as to provide recommendations on appropriate PERS composition. To this end, 20 PERS mixtures with different compositions were designed and characterized after various stages of polishing applied by the Aachener-Raveling-Tester (ARTe). The ravelling resistance of PERS was quantified by measuring the material loss after polishing, while their acoustic performance and rutting resistance were also tested for validation purpose. It was concluded that binder content and degree of compaction are the critical factors affecting the ravelling resistance of PERS. To ensure sufficient durability, a minimum binder content of 15% and a minimum compaction degree of 98% were recommended.

[1] Institute of Highway Engineering Aachen, RWTH Aachen University, Germany

[2] Federal Highway Research Institute, Germany

[3] The Hong Kong Polytechnic University, Hong Kong, zhen.leng@polyu.edu.hk (*Corresponding Author)

[4] Harbin University, China

Keywords: Poroelastic road surface; ravelling resistance; polishing resistance, acoustic properties

1. INTRODUCTION

The continuous development of low-noise porous asphalt (PA) pavement has led to the invention of Poroelastic Road Surfaces (PERS), which is mainly composed of tyre rubber granules, polyurethane, some supplemental materials, such as sand, rocks or other friction-increasing additives, and large air void (up to 40%) [1-6]. The noise reduction function of PA pavement mainly relies on its larger air void contents (18% to 25%) compared with conventional asphalt pavements. Compared with PA, PERS has even higher air void content. In addition, high amount of rubber particles are used in PERS, making it highly elastic and extremely porous, therefore providing even better tyre-road noise reduction performance compared with PA [1-3]. To improve the bonding between the rubber and aggregate particles, polyurethane is used as the binder in PERS instead of asphalt.

PERS was invented in Sweden in the late 1970's. In the mid 1990's, the Public Works Research Institute (PWRI) in Japan gained interest in the concept and constructed a number of test tracks, which were in service for up to three years. From 2004 to 2008, some PERS test tracks were built in Sweden and the Netherlands, and noise reductions of approximately 8 dB(A) were reported [1-6]. In September 2009, a six-year project named PoroElastic Road Surface to Avoid Damage to the Environment (PERSUADE) was launched to develop PERS from an experimental concept to the stage of a practically usable noise abatement measure [7-9]. Various performances of PERS were investigated in this project, including noise reduction capacity, mechanical and aerodynamic noise excitation, and safety, wearing resistance and durability. The existing studies in Europe and Japan have proved that PERS provided outstanding performance in tyre-road noise reduction. The reported noise reduction achieved by PERS was up to 10-12 dB(A), while the quietest conventional low-noise pavement, two-layer porous asphalt, rarely yields reductions exceeding 7 dB(A) [7-11].

Although PERS exhibits outstanding performance in noise reduction, it also faces the challenging problem of mechanical ravelling, which significantly reduces its service life and limits its wider application [12-13]. As FIGURE 1 shows, the poor ravelling resistance of PERS is mainly caused by its open-graded structure, which does not provide enough granule-to-granule contact surfaces to withstand the imposed shear loading, particularly in the areas of sharp bends or during the processes of braking or accelerating. Thus, it becomes an important but challenging task to ensure adequate ravelling resistance of PERS whilst maintaining its outstanding noise reduction function. Correspondingly, this study aims to investigate the effects of the material composition and compaction on the ravelling resistance of PERS and provide recommendations on appropriate PERS composition which provides balanced ravelling resistance and acoustic performance.

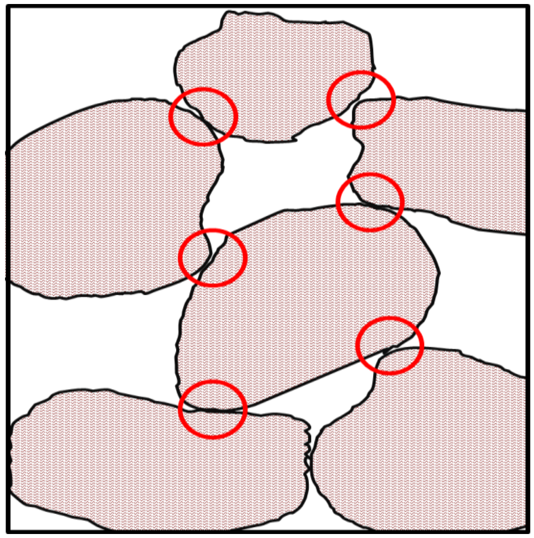

FIGURE 1 Structure of PERS

2. EXPERIMENTAL PROGRAM AND RESEARCH METHODOLOGY

To achieve the objective of this study, the following two research tasks were conducted:

1) optimizing the composition of PERS in terms of its ravelling resistance; and

2) validating the acoustic performance and rutting resistance of the selected PERS from Task 1, and comparing them with those of the conventional road surface materials. The following provides the details of the experimental program and research methodology.

2.1 Ravelling Resistance

Based on the experiences in Sweden, Norway, Japan and the Netherlands, the ravelling resistance of PERS is mainly affected by the following factors: coarse rubber granule content, fine rubber granule content, quartz sand content, binder content, and degree of compaction [1-6]. Thus, the effects of these variables on PERS's ravelling resistance were investigated in this study.

According to the findings in literature, four compositions as shown in Table 1 were designed and evaluated in this study. In this table, the contents of quarts sand and rubber granules were calculated based on the total weight of sand and rubber granules. For each composition, five different compaction degrees were considered, leading to 20 PERS variants in total. Variations of the compaction degree, k, were achieved by adjusting the rolling compaction numbers in the manual manufacturing process. The final measured compaction degrees of the test samples were within the range of 85% to 100%. The target air void content of PERS was 35%. In other words, the actual air void contents varied from 29.8% to 35.0%. The sizes of fine rubber granules and coarse rubber granules were 0.2-0.8mm and 3.1-6.0mm, respectively. The polyurethane product Elastopave® 6551/102 supplied by BASF Polyurethanes GmbH (Lemförder, Germany) was selected as the binder. It is a two component commercial polyurethane binder specially designed for pavement applications. The two components of the binder are polyol mixture (A-component) and diphenylmethane diisocyanate (B-component). Figure 1 shows the pictures of the major components of PERS as well as a compacted PERS sample.

TABLE 1 Test matrix for the contents of the main PERS components

Binder, B	Quartz Sand (0-2.0mm), Q	Total Rubber $G_f + G_c$	Fine Rubber Granules (0.2-0.8mm), G_f	Coarse Rubber granules (3.1-6.0mm), G_c
10	15	85	5	80
15	15	85	5	80
10	2	98	8	90
15	2	98	8	90

Note: All contents are given in M.-%

a)

b)

c)

d)

FIGURE 2 Components and Test Sample of PERS: (a) Fine rubber granules; (b) Coarse rubber granules, (c) Polyurethane binder; (d) PERS sample

The ravelling resistance of PERS was evaluated by measuring the granule loss after various stages of polishing: 0min, 5min, 10min, 20min, and 40min, applied by the advanced Aachener-Raveling-Tester (ARTe). As shown in FIGURE 3, the ARTe is a polishing machine equipped with real vehicle tires (Type: Vanco 8, 165/75 R 14 C 8PR 97/95 R TL from Continental). It applies shear stress to test plates by superposing translational and rotational motions. A horizontally movable sled carrying the samples is responsible for the translational motion, while two wheels rotating around a vertical axis induce the rotational motion. The tires are inflated with an inner pressure of 0.2 MPa and carry a load of 200 kg. The sled moves back and forth horizontally 9 times/min while the tires spin 41 rotations/minute. The diameter of the circular path made by the rotating tires is 55 cm. Therefore, the velocity of the circular motion is about 1.2 m/s. With such configuration, the entire test plate is subjected to an equal polishing effect [14-16]. FIGURE 4 shows a standard ARTe test sample measuring 260mm x 320mm x 40 mm. It was prepared by compacting a 16mm-thick PERS layer onto a 24mm-thick concrete base layer through a manual rolling process [3].

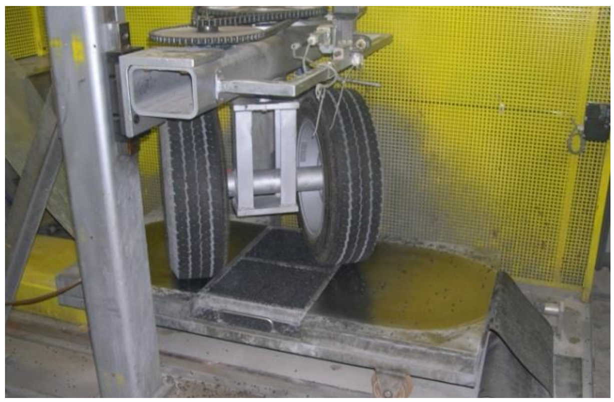

FIGURE 3 Aachener-Ravelling-Tester (ARTe)

FIGURE 4 Standard ARTe test sample

The granule loss after each polishing stage is described by Δh in cm calculated by the following equation [22]:

$$\Delta h = h_0 \cdot (1 - \frac{M_t}{M_0})$$

where

h_0: initial height [cm];

M_0: initial weight of the test plate [g];

M_t: weight of the test plate after a polishing duration of *t* minutes [g];

t: polishing duration [min].

A higher granule loss corresponds to a lower ravelling resistance.

2.2 Acoustic Performance

Based on the ravelling resistance test results, the PERS mixture exhibiting the best ravelling resistance was identified and its acoustic performance was further characterized

Tyre-road noise is the consequence of the superposition of several uncorrelated sound sources. Each sound source is related to a particular sound generation mechanism, which include:

- Tyre vibrations due to the excitation of the tyre structure ($p_{vibration}$)
- Airflow related mechanism due to aerodynamic processes in the contact zone ($p_{airflow}$)
- The radiation from interior resonances of the cavity between tyre structure and frim cavity (p_{cavity})
- Flow noise due to the flow around the vehicle body ($p_{vehicle}$)
- Friction and addition effects ($p_{friction}$)

The total tyre-road noise (ptotal) has the following relationship with the above sounds:

$$p^2_{total} = p^2_{vibration} + p^2_{airflow} + p^2_{cavity} + p^2_{vehcile} + p^2_{friction}$$

In this study, the acoustic performance of PERS samples were characterized by measuring its acoustic absorption, air flow resistivity, and mechanical impedance, which are the three major factors affecting the tyre-road noise, corresponding to the abovementioned p_{cavity}, $p_{airflow}$, and $p_{vibration}$, respectively.

2.2.1 Acoustic Absorption

The acoustic absorption of PERS was measured by the impedance tube test in accordance with EN ISO 10534-2: “Acoustics - Determination of sound absorption coefficient and impedance in impedance tubes – Part 2: Transfer-function method (ISO 10534-2:1998)”.

As FIGURE 5 illustrates, the impedance tube is a straight rigid smooth and air-tight tube, fitted with a speaker on one end and the sample at the other end. The sample holder is a separate unit which is attached to the tube for measurement. The diameter of the samples, which is the same as the inside diameter of the impedance tube, was 50 mm in this study. The sample holder can be adjusted to the height of the sample by means of a piston and was set to be level with the bottom side of the sample to prevent any cavities, thus creating an acoustically hard end point. The impendence tube has an acoustically hard inner lining, forcing the sound to propagate in the longitudinal direction. If the diameter of the tube is small relative to the wave length, the sound waves propagate only in longitudinal direction [18].

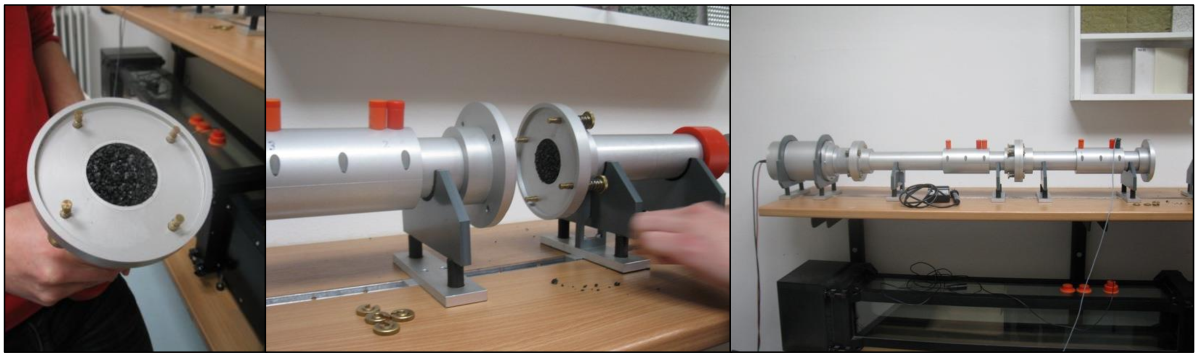

FIGURE 5 Setup of the impedance tube for measuring absorption properties of material samples: (a) PERS sample in the holder: (b) attaching sample holder to the tube; (c) outside appearance of the whole device [19]

The speaker sweeps through a given frequency range, creating plane waves in the tube. The sound pressure is measured at two points in close proximity to the sample by means of microphones attached to the tube wall. The complex acoustical transfer functions of the two microphone signals are determined and used to calculate the complex reflection factor, absorption factor and the acoustic impedance of the sample material (in accordance with EN ISO 10534-2).

The absorption factor is given as a function of the frequency. The applicable frequency ranges may be adjusted by varying the diameter of the tube and/or varying the distance between the microphones (according to EN ISO 10534-2).

2.2.2 Air Flow Resistivity

Air flow resistivity is important for aero dynamic effects in the tyre-road contact patch as well as the absorption characteristics. Different pavement mixtures usually have different air void structures and sizes. The distribution, interconnectivity, size and shape of air voids all affect the air flow resistivity. To minimize the tyre-road noise, a relatively low air flow resistivity is desired. This may be achieved by an inter-connected air void structure in combination with a sufficient air void content. In this study, the experimental setup (AFD 300 – AcoustiFlow®) as shown in FIGURE 6 was used. The air flow resistivity was determined by means of a continuous air flow method, where a laminar air flow runs through the sample and the pressure loss is measured. In this study, the setup was slightly altered compared with the specifications in DIN EN 29053/ISO 9053. A cylindrical bushing with an inner diameter of 100 mm was placed on top of the sample with an imposed load of 60 kg. This setup allows for the determination of the effective specific air flow resistivity, which is independent of the layer thickness [21]. The specific air flow resistivity was measured at numerous air flow speeds for each sample. Finally, the air flow resistivity was determined at a flow velocity of 12.5 mm/s by means of linear regression [17, 21].

FIGURE 6 Setup of the measurement equipment to determine the specific air flow resistivity

2.2.3 Mechanical Impedance

Mechanical impedance of pavement material directly affects the mechanical vibration of tyres caused by the tyre-road interaction. From the acoustic point of view, elasticity and air void content are the main characteristics in which PERS differs from the conventional porous asphalt. The incorporation of rubber granules leads to higher elasticity which in turn results in lower vibration excitation of the tyre. The mechanical impedance can be described in analogy to the acoustic impedance. It describes the resistance of propagating waves from one medium to another; i.e., pavement to tyre in this case. A lower impedance of the pavement surface allows for more energy dissipated in pavement surface, resulting in reduced tyre-road noise induced by the mechanical excitations of the tyre.

As FIGURE 7 shows, the mechanical impedances of PERS samples were measured by an electro mechanical shaker with an imposed static load of 26 kg via a 60mm-diameter loading plate, in accordance with ISO 10534-2: Acoustics -- Determination of sound absorption coefficient and impedance in impedance tubes -- Part 2: Transfer-function method. The force and acceleration of the impedance-device was measured, followed by the computation of the mechanical input impedance with software.

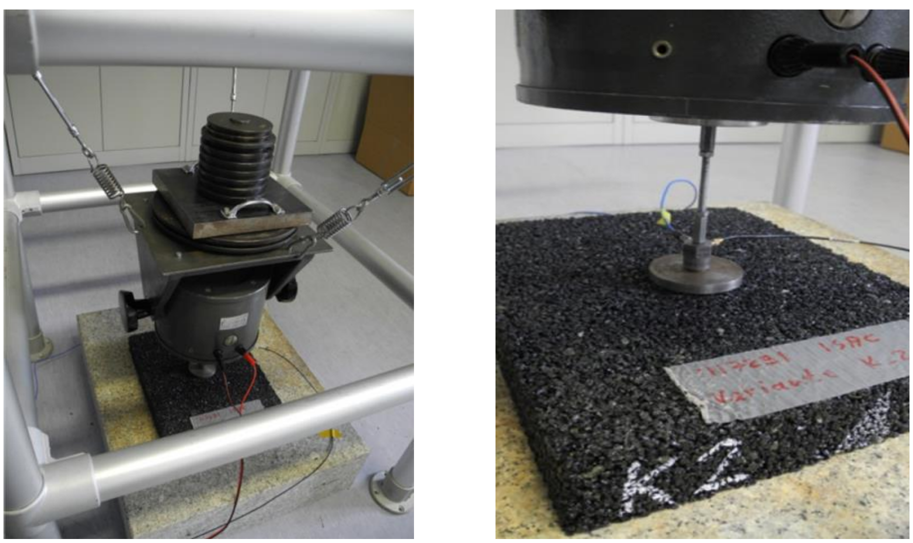

FIGURE 7 Determining the mechanical input impedance with electro mechanical shaker

2.3 Rutting Resistance

As FIGURE 8 shows, the rutting resistance of the PERS samples was assessed by the wheel tracking test in accordance with “Specifications for testing asphalt mixes, part: wheel tracking test carried out in water with steel wheels” [20]. This test applies repeated loading to test samples with a steel wheel, which rolls back and forth with an imposed load of 700 N. The test can be conducted on two slabs simultaneously which measure 32 cm x 26 cm x 4 cm. The samples are submerged in water at 50°C before and during the test. The rut depth and the corresponding loading cycles are recorded and used to evaluate the material’s high-temperature stability. The test is discontinued at 20,000 cycles or upon measuring a rut depth of 20 mm.

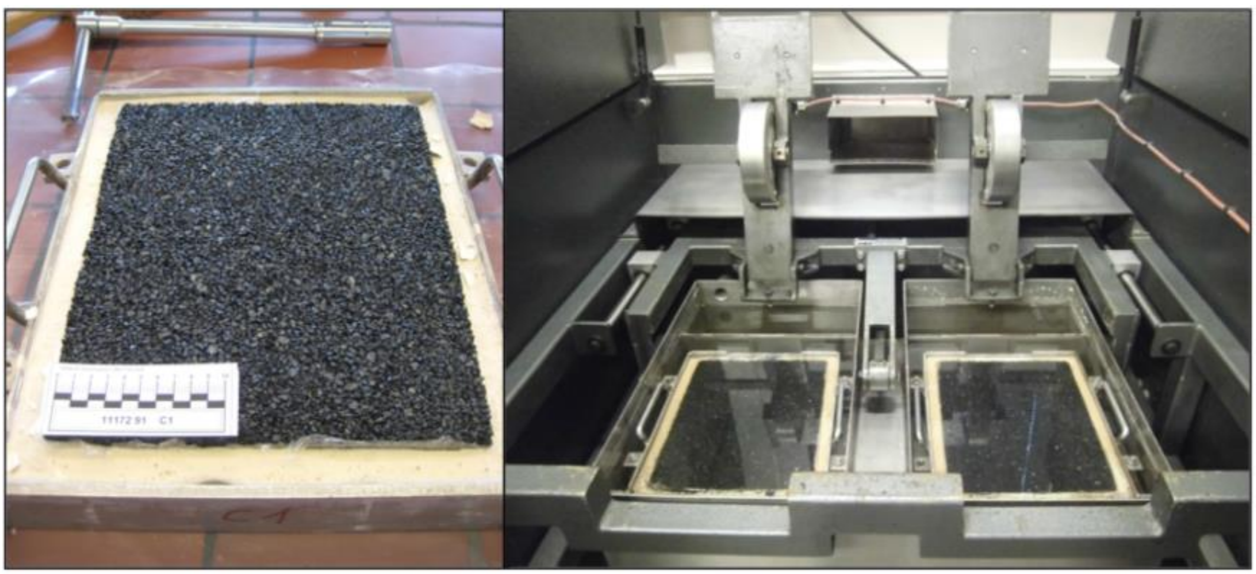

FIGURE 8 Wheel tracking test device

3. RESULTS AND ANALYSIS

3.1 Ravelling Resistance

To determine the most influential factors and their quantitative contributions to the ravelling resistance, a correlation analysis was conducted on each variable at four polishing stages. Table 2 presents the correlation analysis results, which indicate that binder content and compaction degree are the two most significant factors, in addition to the polishing duration, affecting the ravelling resistance, while the effects of other factors are insignificant. Thus, multiple linear regression analysis was further conducted on the ravelling test results by taking into account of polishing duration, t, compaction degree, k, and binder content, B. As a result, the following regression function with a R^2 of 0.872 was derived:

$$\Delta h = 2.250 + 0.25 \cdot t - 0.15 \cdot k - 0.54 \cdot B$$

where

t: polishing duration [s];

k: rate of compaction [%];

B: binder content [%]

The results make it evident that granule breakout rate decreases with an increasing load duration and can be reduced by increasing the compaction degree and binder content. However, contrary to the findings in some literature [1-4], no significant influence of the rubber granule content (coarse and fine) and the quartz sand content could be proved based on the regression analysis.

Table 2 Correlation analysis: influence of composition and compaction degree on Δh

		Binder content	Quartz content	Fine rubber content	Coarse rubber content	Polishing duration	Compaction degree
Δh	Correlation according to Pearson	-.379**	-.034	.034	.034	.835**	-.267*
	Significance (double sided)	.001	.763	.763	.763	.000	.017

Figure 9 illustrates the typical development of granule loss over the polishing duration. In this figure, the granule losses of two PERS mixtures: one with a binder content of 10% and the other with a binder content of 15%, are compared. Both mixtures had the same compaction degree of 94%, and same contents of rubber granules and quartz sand. It is evident in Figure 9 that the granule loss rates of both PERS mixtures decrease over polishing time. However, the PERS mixture with higher binder content exhibits less granule loss throughout the whole polishing process. Thus, it can be concluded that increasing binder content is beneficial for the ravelling resistance of PERS.

FIGURE 10 depicts the granule losses of the PERS mixtures with four compaction degrees: 86%, 92%, 94%, and 98%. All these mixtures had the same material composition: a binder content of 15%, a rubber granule content of 85%, and a quartz sand content of 15%. The results clearly show that for the PERS mixtures with the same composition, a higher degree of compaction leads to a lower granule loss or better ravelling resistance.

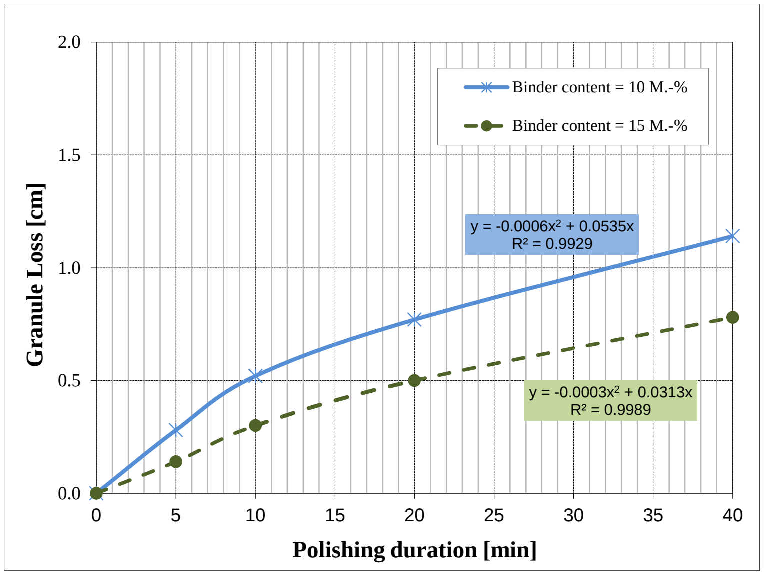

FIGURE 9 Granule losses at different binder contents (k=94 %)

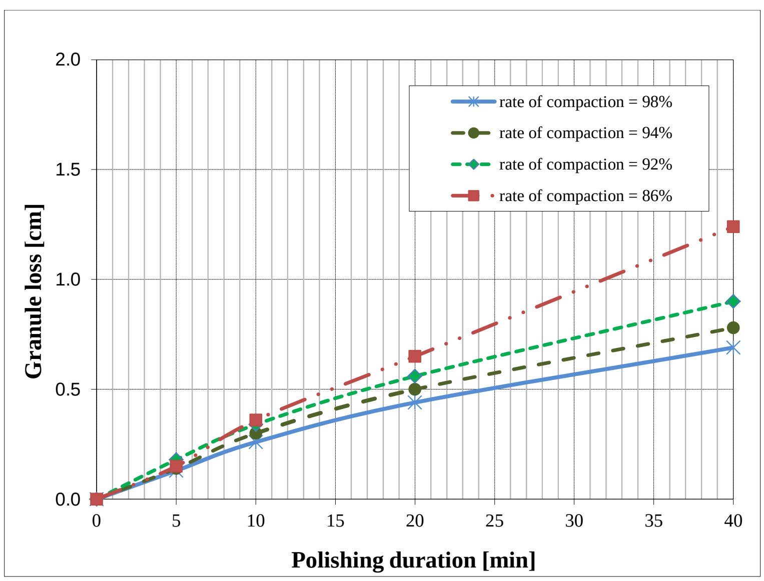

FIGURE 10 Granule loss in relation to the rate of compaction (B=15 %)

3.2 Acoustic Performance

The ravelling test results indicated that a binder content of 15% provides better ravelling resistance than 10%. Besides, previous tests indicated that a quartz sand content of 15%

exhibited more favourable long term skid resistance compared with 2% [21]. Thus, the PERS mixture with a binder content of 15% and 15% of quarts sand (85% of rubber) was selected for further acoustic performance analysis. Three replicates were prepared for the acoustic performance tests.

3.2.1 Absorption Properties

FIGURE 11 shows the absorption coefficients of the PERS samples in comparison to that of a conventional porous asphalt mixture with a maximum aggregate size of 8 mm (PA 8). It can be seen that the absorption coefficients of the PERS samples are within the range of 60% to 95% between 800 Hz and 2500 Hz, the crucial frequency range to human auditory perception. From 200 Hz to 6000 Hz, PERS shows two maximum absorption coefficients: 95% and 82%, at 1500 Hz and 4000 Hz, respectively. The general courses of the absorption coefficients correspond well with the measurements reported by the study conducted in Stockholm [5-6]. The maximum absorption coefficients of PERS (approximately 95%) are significantly higher than that of the reference variant, which is 78%.

Table 3 Mix design of PA 8

Aggregates	Composition	Grain size	Mass percent and Stone type
		<0.063 mm	4.0 M.-%, Limestone

		0.063-2 mm	4.0 M.-%, Diabase
		2-5.6 mm	2.0 M.-%, Diabase
		5.6-8 mm	85.0 M.-%, Diabase
		>8 mm	5.0 M.-%, Diabase
	Apparent density of the mineral grains		2.820 g/cm^3
	Polished stone value (PSV, EN 1097-8: 2009)		58 (Diabase)
Binder	Polymer modified bitumen 40/100-65 A, 6.5 M.-%		
Asphalt mixture	Apparent density of the asphalt mixture 2.541 g/cm^3		
	Air void percentage 26.2 Vol.-%		

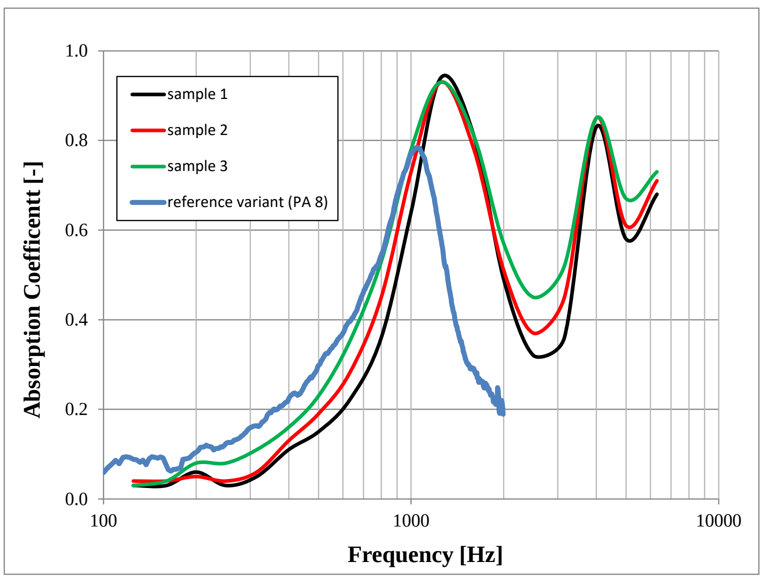

FIGURE 11 Absorption coefficient curves measurements in accordance with ISO 10534-2

It is worth noting that the precise frequency corresponding with the maximum absorption coefficient is a function of the layer thickness, and is not material dependent. In addition to the absolute values of the maximum absorption coefficient, it is important to compare the course of the absorption coefficient over the frequency. To better compare the absorption coefficients, the respective curves were translated vertically and horizontally to match their respective maximum values, as shown in FIGURE 12. It can be seen that the PERS samples exhibit wider maximum peaks compared with the reference variant, which is also an indicator of better noise absorption.

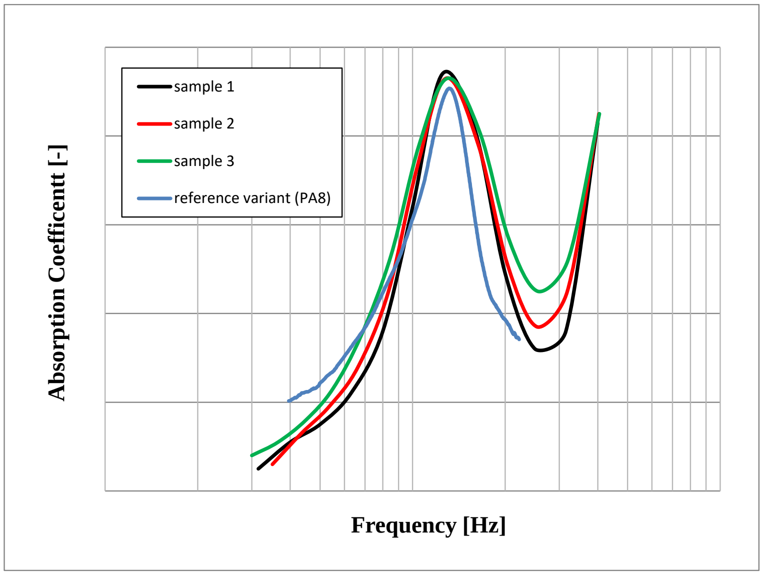

FIGURE 12 Offset absorption coefficient curves to enable better comparison

3.2.2 Air Flow Resistivity

FIGURE 13 presents the effective air flow resistivities of the PERS samples at a flow velocity of 12.5 mm/s along with their measured air void contents. It can be seen that the effective specific air flow resistivities are within the range of 135 to 549 Pa*s/m. The discrepancies can be due to the different air void contents caused by the manual manufacturing process. Among the three PERS samples, sample 1 has the lowest resistivity and the highest air void content. On one hand, a low effective specific air flow resistivity compensates the pressure gradients within the tyre-road contact patch, thus reducing aerodynamic noise generation; on the other hand, a very low effective specific air flow resistivity may lead to a reduced width of the maximum peak pulse of the absorption coefficient and a lower minimum absorption coefficient. This may be the reason why sample 1 exhibits the lowest effective specific air flow resistivity and also the lowest minimum absorption coefficient (Figure 11). As comparison, it was reported that PA 8 surfaces yielded air flow resistivity between 240 and 11,000 Pa*s/m in the middle of wheel tracks and between 380 and 21,000 Pa*s/m in the wheel track, depending on the age of the surface [23]. Thus, the air flow resistivities of the PERS samples tested in this study are close to the lower measured values of the field PA 8 surfaces. However, to further lower the noise emission of PERS, optimization of the gradations of aggregate and rubber granules in terms of the noise absorption and air flow resistivity is recommended.

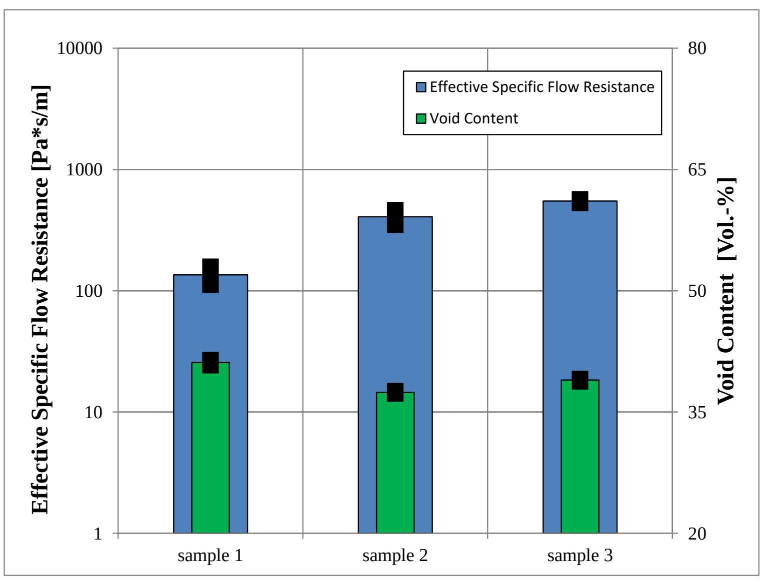

FIGURE 13 Air void content and effective specific air flow resistivity for a flow velocity of 12.5 mm/s

3.2.3 Mechanical Impedance

FIGURE 14 presents the measured mechanical impedances of the three PERS replicates, in comparison to stone mastic asphalt (SMA 5S), which is a conventional asphalt mixture commonly selected as reference for analysing the acoustic properties of wearing courses. It can be seen that the PERS samples exhibited significantly lower mechanical input impedances than the SMA 5 S. A low resistance against the excitation of mechanical vibrations and the resulting dissipation of vibrational energy is most evident at the frequencies below 1000 Hz. Based on the results, a significantly lower resistance against vibrational excitation of the tyre can be achieved by all PERS samples.

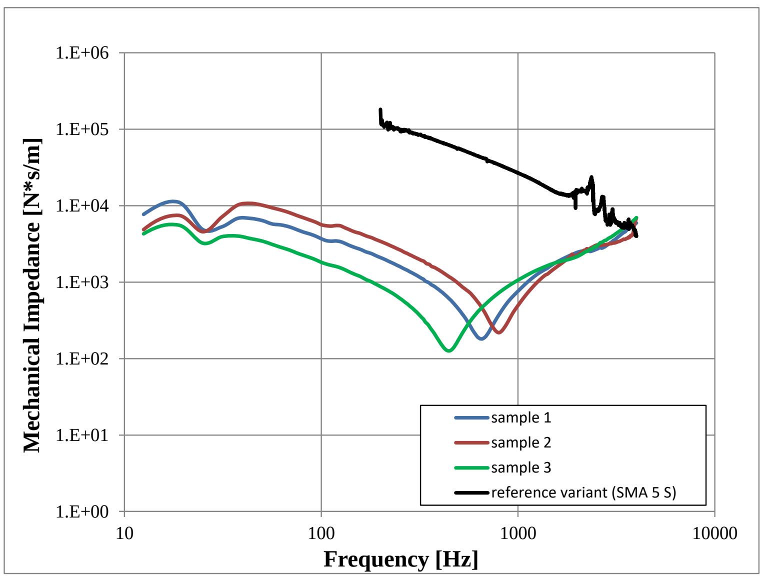

FIGURE 14 Mechanical impedance of the tested samples

3.3 Rutting Resistance

FIGURE 16 and Figure 15 present the pictures of the PERS and PA8 samples after wheel tracking tests and the wheel tracking test results of the two types of mixtures, respectively. It is evident that PERS mixtures provided much better rutting resistance compared with the conventional low-noise pavement material, PA 8. The rutting depths of the PA 8 are approximately 10 times of those of PERS mixtures, which is a result of the profound elasticity arising from the incorporated rubber granules.

FIGURE 16 Images of the samples after the wheel tracking test: PERS (left) and PA 8 (right)

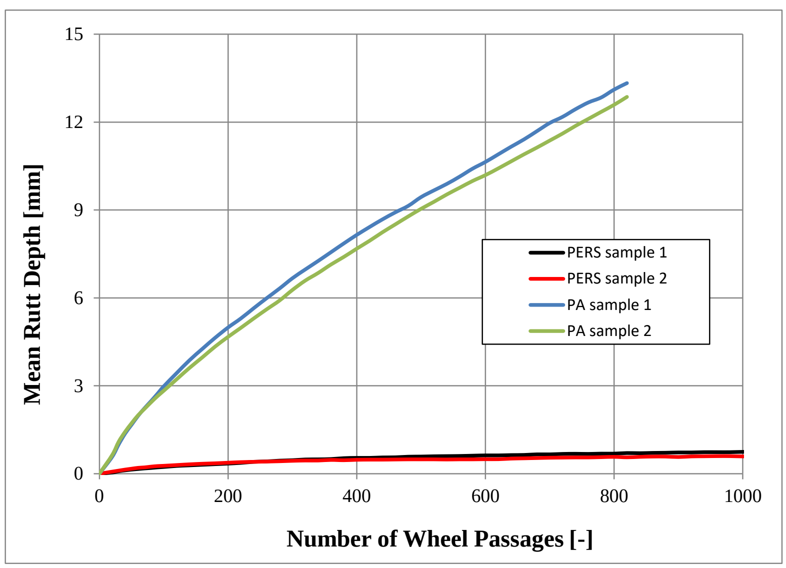

FIGURE 17 Wheel tracking test results of PERS and PA 8

4. FINDINGS AND RECCOMMENDATIONS

This study evaluated the effects various composition factors on the ravelling resistance of PERS, and validated the acoustic performance and rutting resistance of a selected PERS mixture. The following summarizes the major findings of this study:

- With the progressing of shear loading, the rate of granule loss decreases.
- Binder content has the most significant effect on granule loss under polishing: a higher binder content leads to better ravelling resistance.
- Degree of compaction is important to the granule loss under polishing: the ravelling resistance increases with the increase of compaction degree.
- Contrary to the findings in literature, the granule loss was found not significantly affected by rubber granule content and quartz sand content.
- The selected PERS mixture with 15% binder content, and 15% of quartz sand and 85% rubber granule, showed satisfactory acoustic performance and rutting resistance, in comparison to conventional low-noise pavement mixture.

Based on the above findings, it is recommended to use a binder content of at least 15% for PERS mixture in order to guarantee sufficient ravelling resistance, particularly in intersections and bends. Meanwhile, achieving a minimum compaction degree of 98% is recommended to ensure sufficient durability of PERS mixture. Further research is necessary to determine the optimum binder content and optimum rubber and sand gradation to minimize the effective specific air flow resistivity.

ACKNOWLEDGMENTS

The authors acknowledge the sponsorship of the German Research Foundation (DFG) on the work presented in this paper through Research Grant OE 514/4-1.

REFERENCES

[1] Sandberg, U., Goubert, L., Biligiri, K., Kalman, B. (2010). State-of-the-art regarding poro-elastic road surfaces

[2] FEHRL Report 2006/02 (2006). Guidance manual or the implementation of low-noise-road surfaces

[3] Amundsen, A., Klaeboe, R. (2005). A Nordic perspective on noise reduction at the source. Institute of Transport Economics, report 806/2005

[4] Meiarashi, S. (2003). Porous elastic road surface as an ultimate highway noise measure. The XXIInd PIARC World Road Congress.

[5] Sandberg, U., Kalman, B. (2005). SILVIA Project Report, The Poroelastic Road Surface - Results of an Experiment in Stockholm.

[6] Sandberg, U., Kalman, B., Nilsson, R. (2005). Design guidelines for constuction and maintenance of poroelastic road surface. SILVIA-VTI-005-02-WP4-141005.

[7] Sandberg, U., Goubert, L. (2011). PERSUADE - A European project for exceptional noise reduction by means of poroelastic road surfaces. Inter Noise 2011. Osaka, Japan.

[8] Kalman, B., Biligiri, K. P., Sandberg, U. (2011). Project PERSUADE: Optimization of poroelastic road surfaces in the laboratory. Inter Noise 2011. Osaka, Japan.

[9] Pigasse, G., Jensen, M. P., Bendtsen, H. (2012). Cost-benefit analysis of a poroelastic road surface. EuroNoise 2012. Prag.

[10] Sandberg, U., Goubert, L. (2011). Poroelastic Road Surface (PERS): A review of 30 years of R&D work. Inter Noise 2011. Osaka, Japan.

[11] Biligiri, K.P., Kalman, B., Samuelsson, A. (2013). Understanding the fundamental material properties of low-noise poroelastic road surfaces, International Journal of Pavement Engineering, Vol. 14, No. 1, January 2013, 12–23

[12] Goubert, L., Bendtsen, H., Bergiers, A., Kalman, B., Kokot, D. (2014). The poroelastic road surface (PERS): the 10 dB reducing pavement within reach?, Transport Research Arena 2014, Paris

[13] Goubert, L. (2014). Developing a durable and ultra low noise poroelastic pavement, Inter-noise Conference 2014

[14] Wang, D., Chen, X., Yin, C., Oeser, M., Steinauer B. (2013). Influence of different polishing conditions on the skid resistance development of asphalt surface, Wear, 308, 71–78.

[15] Wang, D., Chen, X. Xie, Stanjek, H., Oeser, M., Steinauer B. (2015). A study of the laboratory polishing behavior of granite as road surfacing aggregate, Construction and Building Materials, Vol 89, 25–35.

[16] Wang, D., Chen, Stanjek, H., Oeser, M., Steinauer B. (2014). Influence of freeze-thaw on the polishing resistance of coarse aggregates on road surface, Construction and Building Materials, Vol 64, 192–200.

[17] Beckenbauer, T., Spiegler, P. (2002). Einfluss der Fahrbahntextur auf das Reifen-Fahrbahn-Geräusch. Forschung Straßenbau und Straßenverkehrstechnik, Heft 847, Bundesministerium für Verkehr, Bau und Wohnungswesen

[18] Möser, M. (2009). Technische Akustik, 8.,aktualisierte Auflage. Berlin: Springer.

[19] Vorländer, M. (2012). Akustisches Praktikum - Die akustische Messleitung (Kundt’sches Rohr). s.l. : Institut für Technische Akustik.

[20] FGSV (1997). TP A-StB, Technische Prüfvorschriften für Asphalt, Teil: Spurbildungsversuch - Bestimmung der Spurrinnentiefe im Wasserbad. Köln: Forschungsgesellschaft für Straßen- und Verkehrswesen (FGSV)

[21] Schacht A. (2015). Entwicklung künstlicher Straßendeckschichtsysteme auf Kunststoffbasis zur Geräuschreduzierung mit numersichen und empirischen Verfahren, Dissertation, Aachener Mitteilungen Straßenwesen Erd-, und Tunnelbau; Institut für Straßenwesen, Aachen

[22] Schacht, A., Wang, D., Steinauer, B. (2011). Untersuchung der Kornausbrüche bei poro-elastischen Fahrbahnbelägen mit dem Aachener Ravelling Tester (ARTe), Bauingenieur 4-2011, S. 160-168, Springer-VDI-Verlag GmbH & Co. KG.

[23] Altreuther, B. and Bartolomaeus, W. (2008). Acoustical characterisation and life-cycle of porous road surfaces. The Journal of the Acoustical Society of America, 2969-2974